Electronic Supplementary Material (ESI) for Inorganic Chemistry Frontiers.
This journal is © the Partner Organisations 2023

Supporting Information

Cancer cell membrane camouflaged and H_2O_2-activatable nanocomposites for synergistic chemotherapy and two-photon photodynamic therapy against melanoma

Siyuan Gao,[a] Fangmian Wei,[a] Johannes Karges,[b] Yukun Zhao,*[c] Liangnian Ji,[a] Hui Chao*[a,d]

[a] *MOE Key Laboratory of Bioinorganic and Synthetic Chemistry, School of Chemistry, Guangdong Provincial Key Laboratory of Digestive Cancer Research, The Seventh Affiliated Hospital, Sun Yat-Sen University, Guangzhou, 510006, P. R. China. E-mail: ceschh@mail.sysu.edu.cn*

[b] *Faculty of Chemistry and Biochemistry, Ruhr-University Bochum, Universitätsstrasse 150, 44780 Bochum, Germany.*

[c] *Department of Dermatology, The Eastern Division of the First Affiliated Hospital, Sun Yat-Sen University, Guangzhou, 510275, P. R. China. E-mail: zhaoyukun7288569@sina.com*

[d] *MOE Key Laboratory of Theoretical Organic Chemistry and Functional Molecule, School of Chemistry and Chemical Engineering, Hunan University of Science and Technology, Xiangtan, 400201, P. R. China.*

Table of Contents

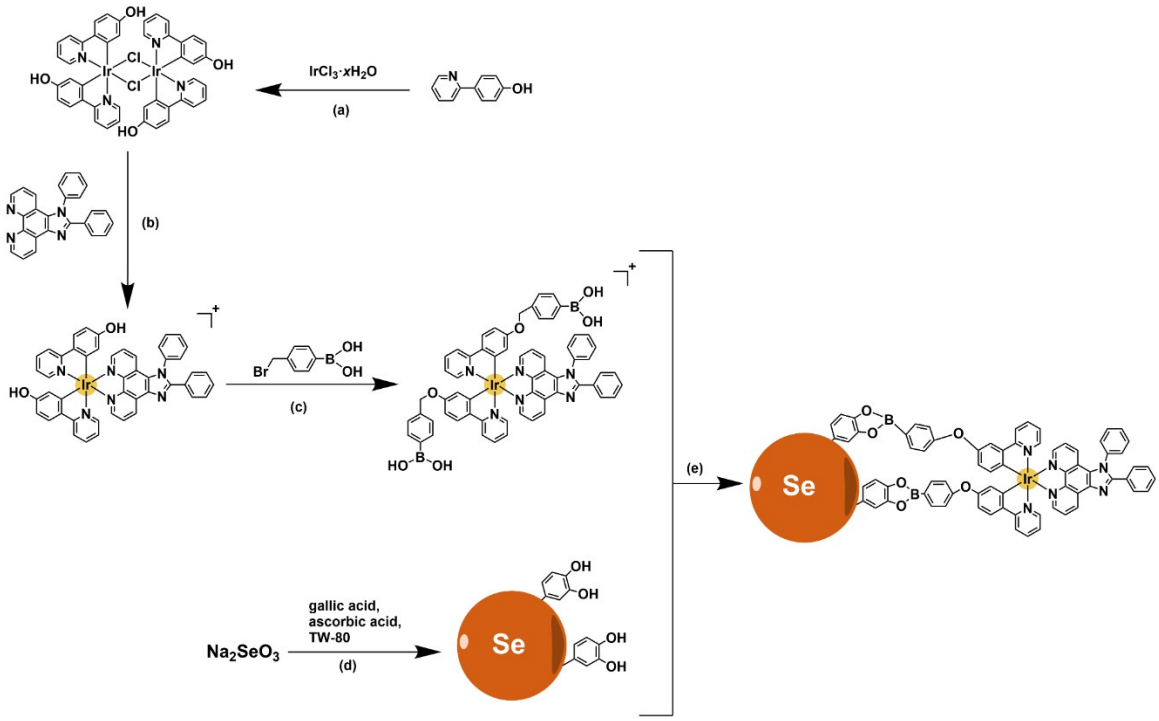

Scheme S1. Synthesis of **Ir-OH, Ir-B(OH)$_2$**, and **Ir@SeNPs**. (a) 2-Ethoxyethano, H_2O, dark, Ar atmosphere, 125°C, 24 h; (b) CH_2Cl_2, CH_3OH, dark, Ar atmosphere, 65°C, 12 h; (c) K_2CO_3, dry DMF, 63°C, 2h; (d) H_2O, room-temperature, overnight; (e) DMSO, H_2O, 37°C, 48 h.

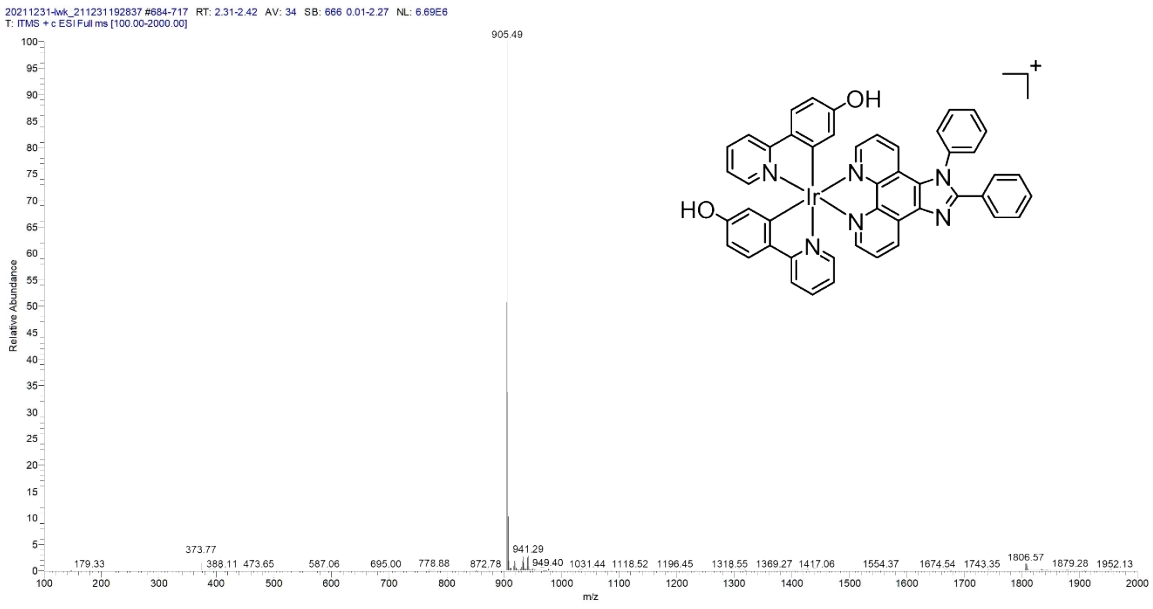

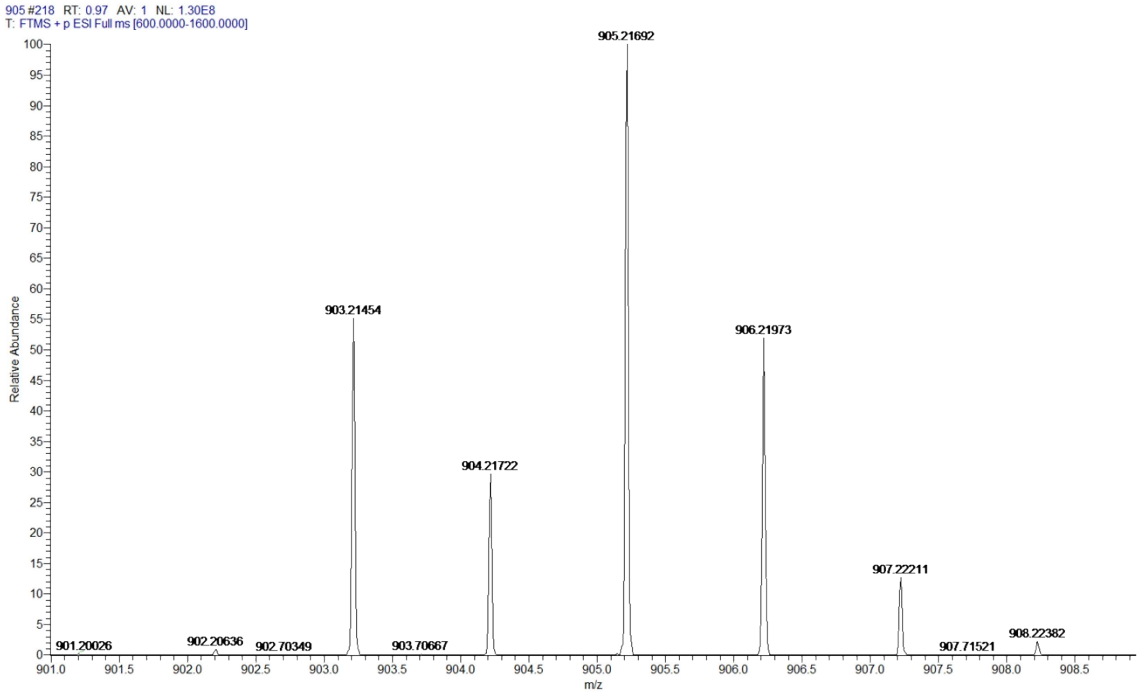

Figure S1. ESI-MS spectrum (top) and HRMS (bottom) spectrum of **Ir-OH**. HRMS, *m*/*z* = $C_{47}H_{32}IrN_6O_2$, 905.2216 $[M]^+$, found, 905.2169 $[M]^+$.

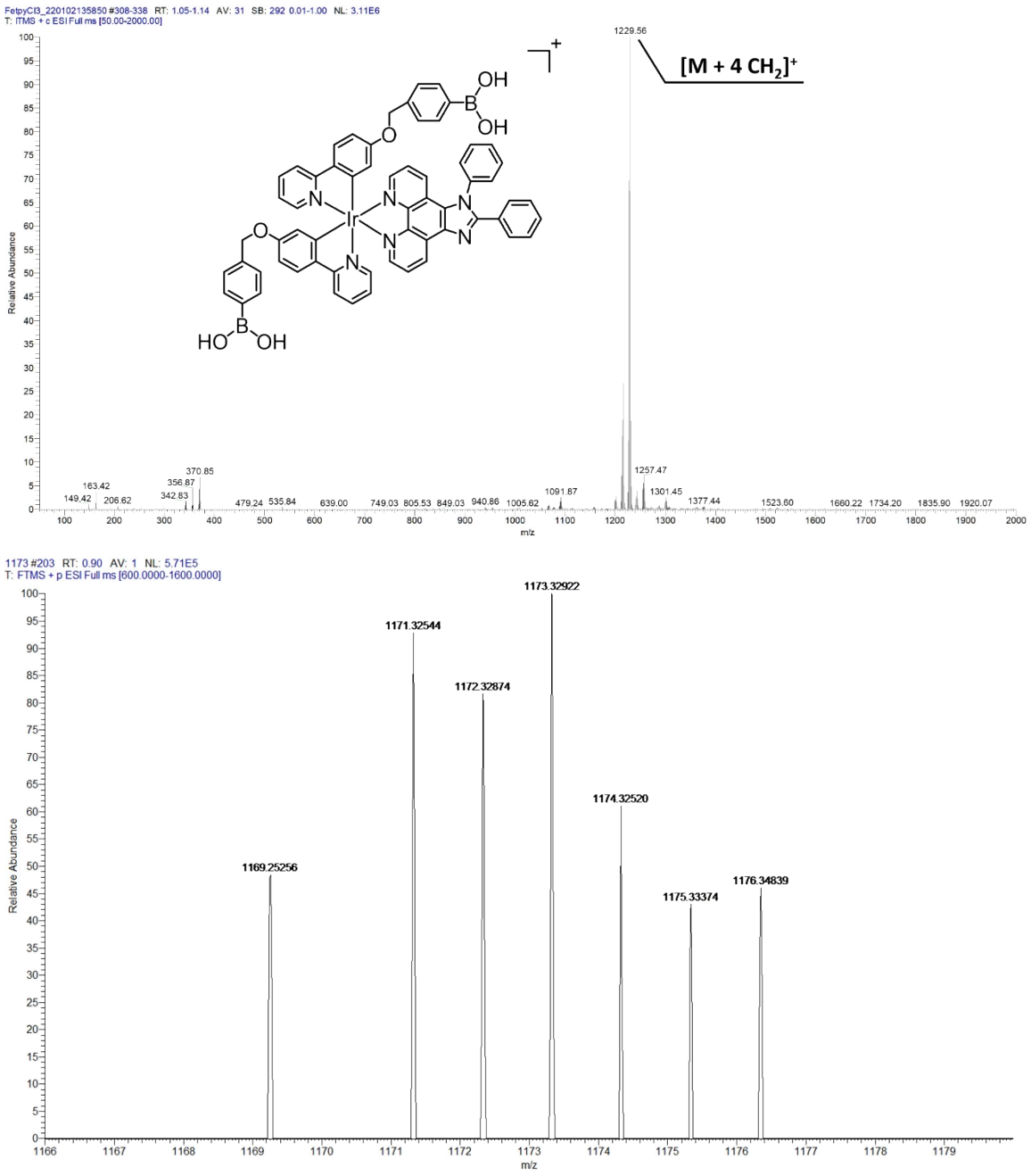

Figure S2. ESI-MS spectrum (top, tetra-methyl boronic ester form) and HRMS (bottom) spectrum of **Ir-B(OH)$_2$**. HRMS, *m/z* = $C_{61}H_{46}B_2IrN_6O_6$, 1173.3294 $[M]^+$, found, 1173.3292 $[M]^+$.

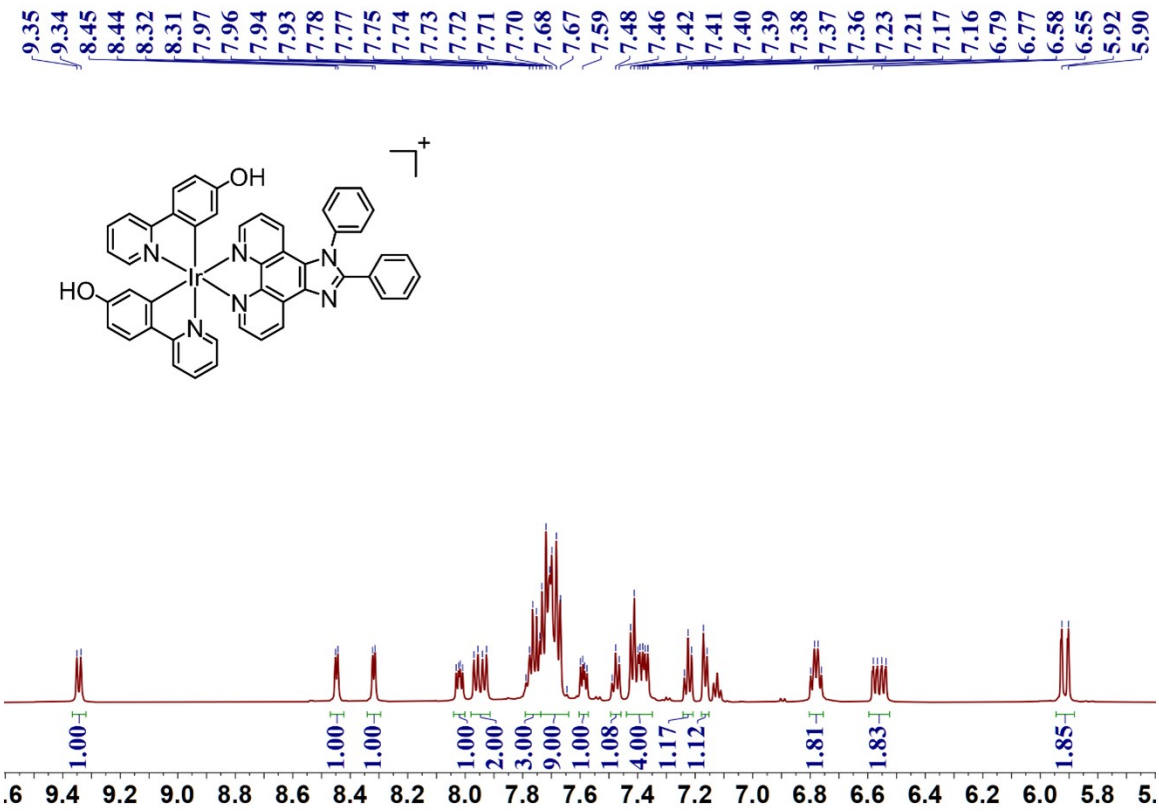

Figure S3. ^{1}H-NMR spectrum of **Ir-OH**. ^{1}H-NMR (600 MHz, Methanol-d_4) δ 9.34 (d, *J* = 8.2 Hz, 1H), 8.45 (d, *J* = 5.1 Hz, 1H), 8.32 (d, *J* = 5.1 Hz, 1H), 8.02 (dd, *J* = 8.4, 5.1 Hz, 1H), 7.95 (m, 2H), 7.76 (p, *J* = 7.1, 6.7 Hz, 3H), 7.70 (m, 9H), 7.59 (dd, *J* = 8.7, 5.0 Hz, 1H), 7.48 (t, *J* = 7.4 Hz, 1H), 7.44 – 7.35 (m, 4H), 7.23 (t, *J* = 7.5 Hz, 1H), 7.17 (d, *J* = 7.5 Hz, 1H), 6.78 (m, 2H), 6.56 (m, 2H), 5.91 (d, 2H).

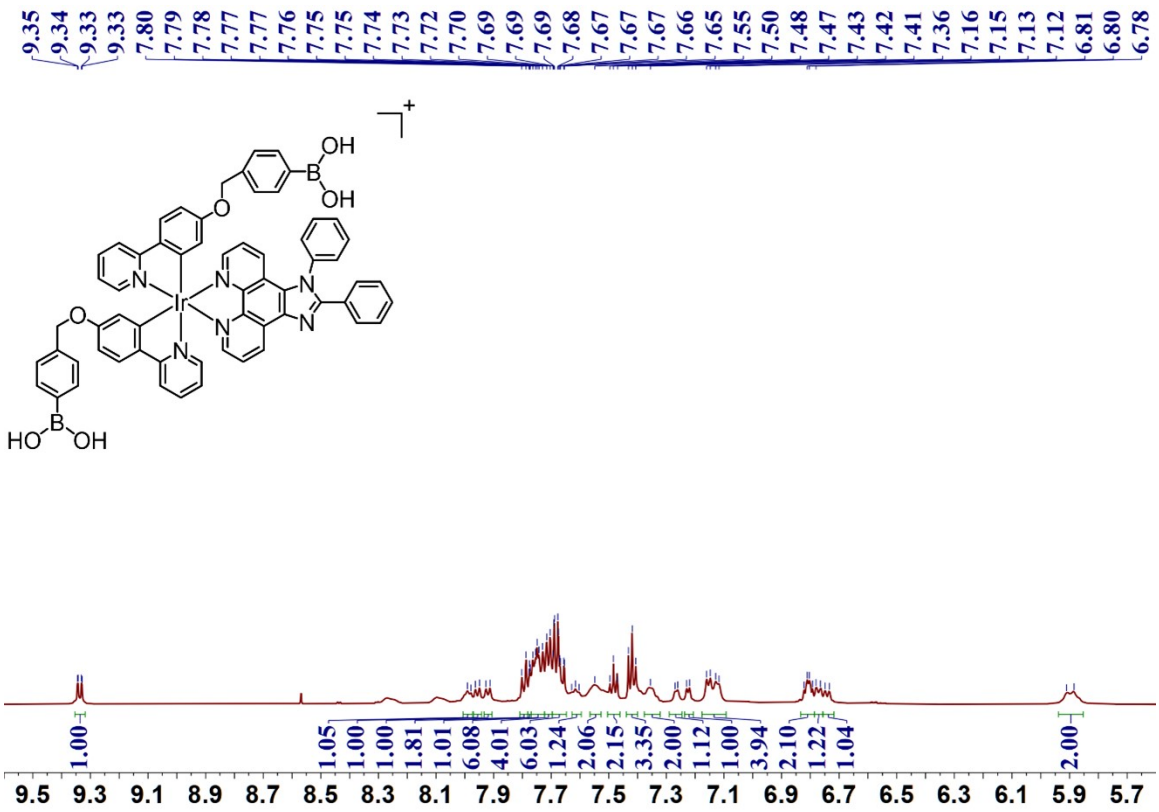

Figure S4. ^{1}H-NMR spectrum of **Ir-B(OH)$_2$**. ^{1}H-NMR (600 MHz, Methanol-d_4) δ 9.34 (dd, *J* = 8.3, 1.5 Hz, 1H), 7.98 (d, *J* = 7.4 Hz, 1H), 7.96 (d, *J* = 8.3 Hz, 1H), 7.92 (d, *J* = 8.2 Hz, 1H), 7.79 (d, *J* = 8.8 Hz, 2H), 7.77 (t, *J* = 1.5 Hz, 1H), 7.77 – 7.72 (m, 6H), 7.71 (d, *J* = 7.1 Hz, 4H), 7.67 (m, 6H), 7.61 (d, *J* = 7.5 Hz, 1H), 7.55 (s, 2H), 7.50 – 7.46 (m, 2H), 7.42 (t, *J* = 7.6 Hz, 3H), 7.36 (s, 2H), 7.27 (d, *J* = 5.8 Hz, 1H), 7.22 (d, *J* = 5.9 Hz, 1H), 7.14 (m, 4H), 6.81 (t, *J* = 5.6 Hz, 2H), 6.77 (d, *J* = 9.3 Hz, 1H), 6.74 (d, *J* = 8.4 Hz, 1H), 5.90 (d, 2H).

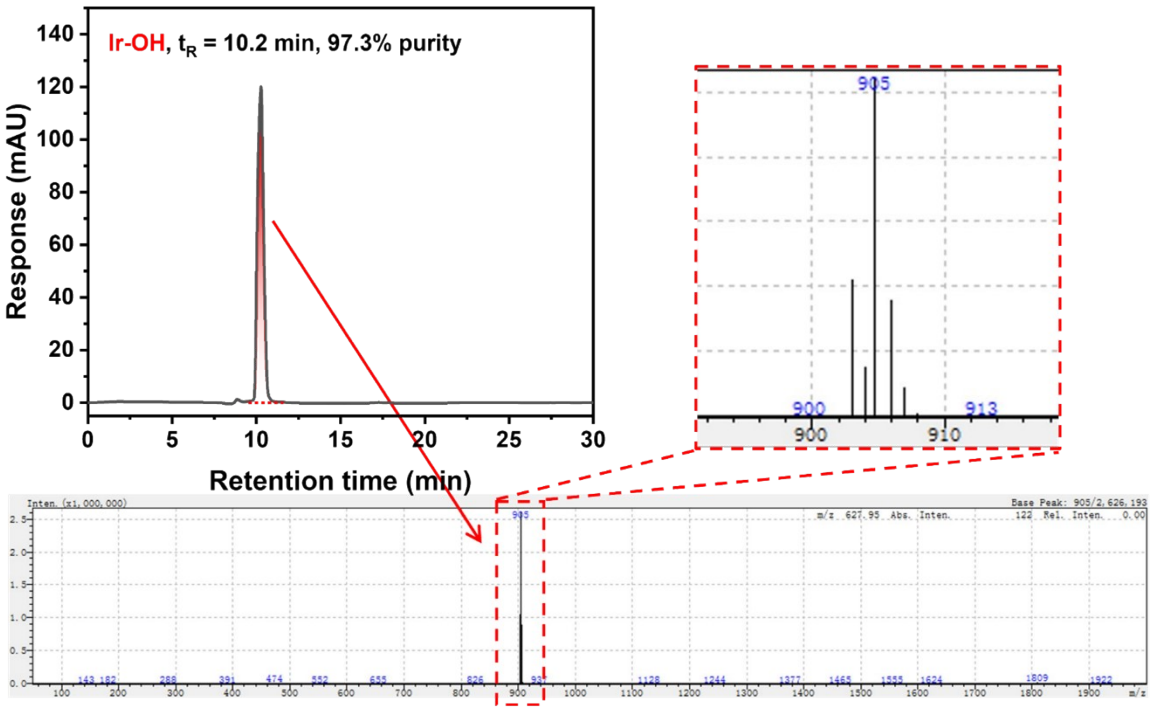

Figure S5. The purity of **Ir-OH** detected by LC-MS (top) and its relative mass spectrogram (bottom). The enlarged part showed the amplified mass spectrogram of **Ir-OH**.

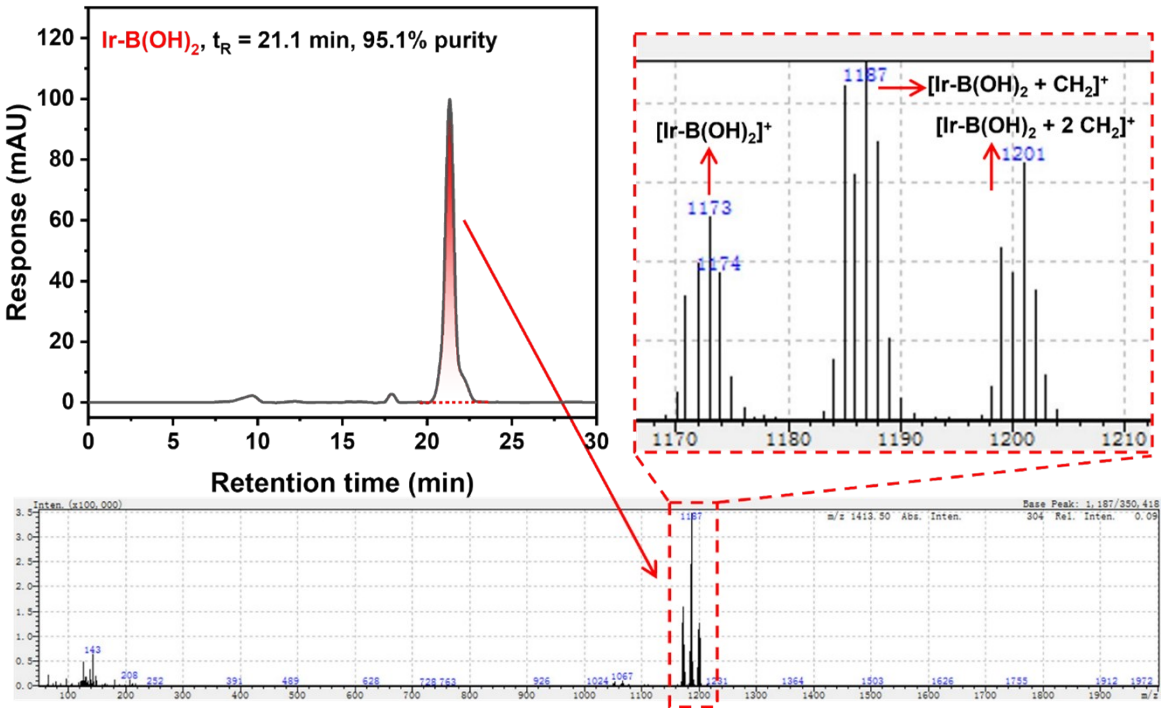

Figure S6. The purity of **Ir-B(OH)$_2$** detected by LC-MS (top) and its relative mass spectrogram (bottom). The enlarged part of the mass spectrogram indicated that the mono-, di, and tri-methyl boronic ester had been formed under the testing condition with CH_3OH.

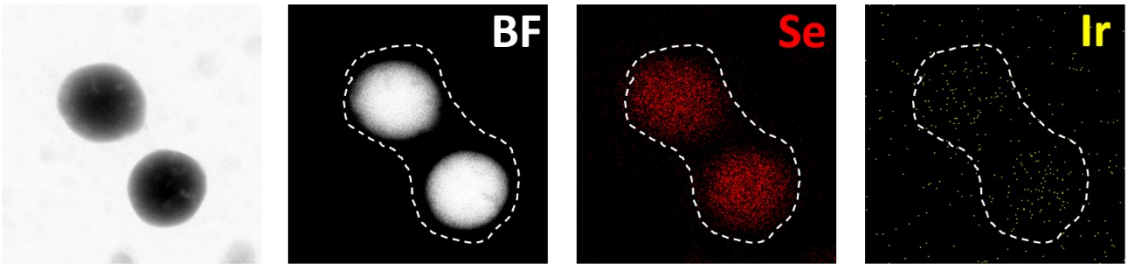

Figure S7. Elemental mapping of **Ir@SeNPs** with the elements Ir or Se marked in different colors.

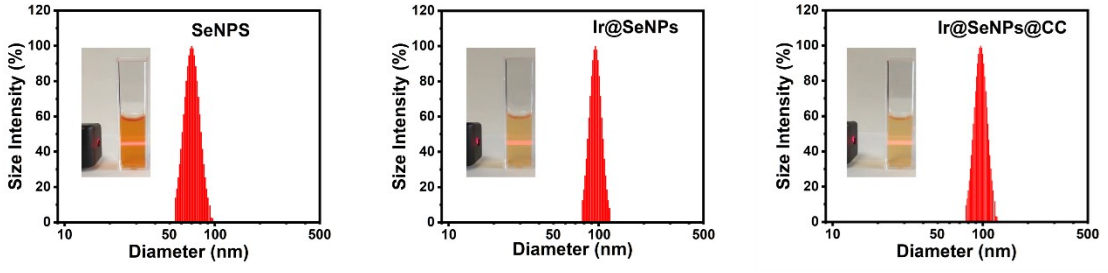

Figure S8. Size distribution of **SeNPs** (76.3 ± 16.8 nm), **Ir@SeNPs** (92.4 ± 17.3 nm), and **Ir@SeNPs@CC** (99.2 ± 20.0 nm) determined by dynamic light scattering.

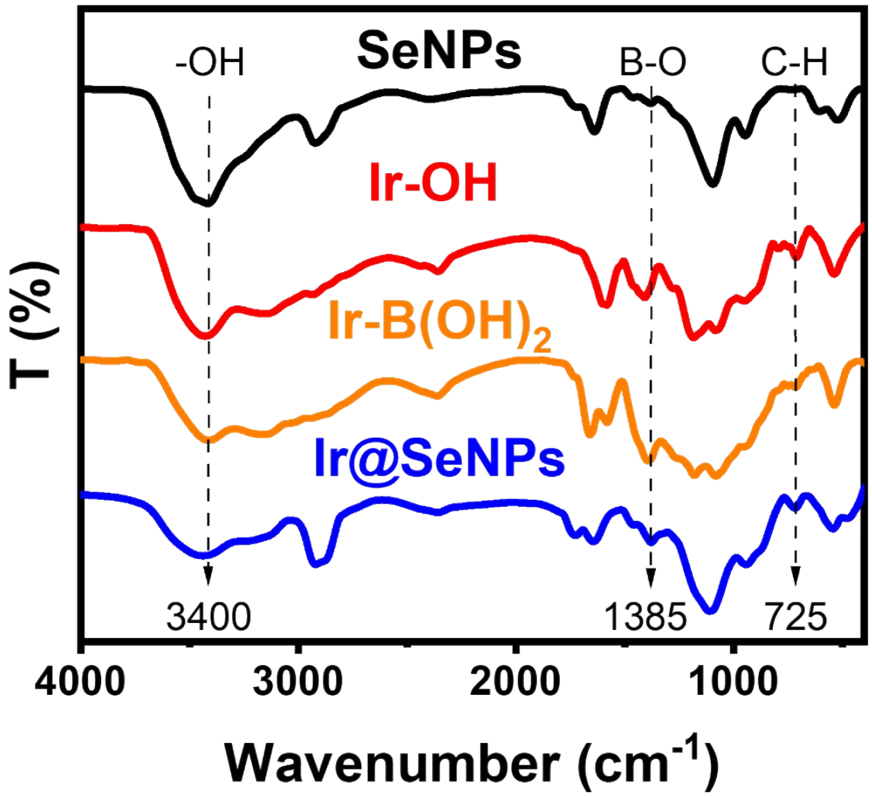

Figure S9. FTIR spectra of **SeNPs**, **Ir-OH**, **Ir-B(OH)$_2$**, and **Ir@SeNPs**.

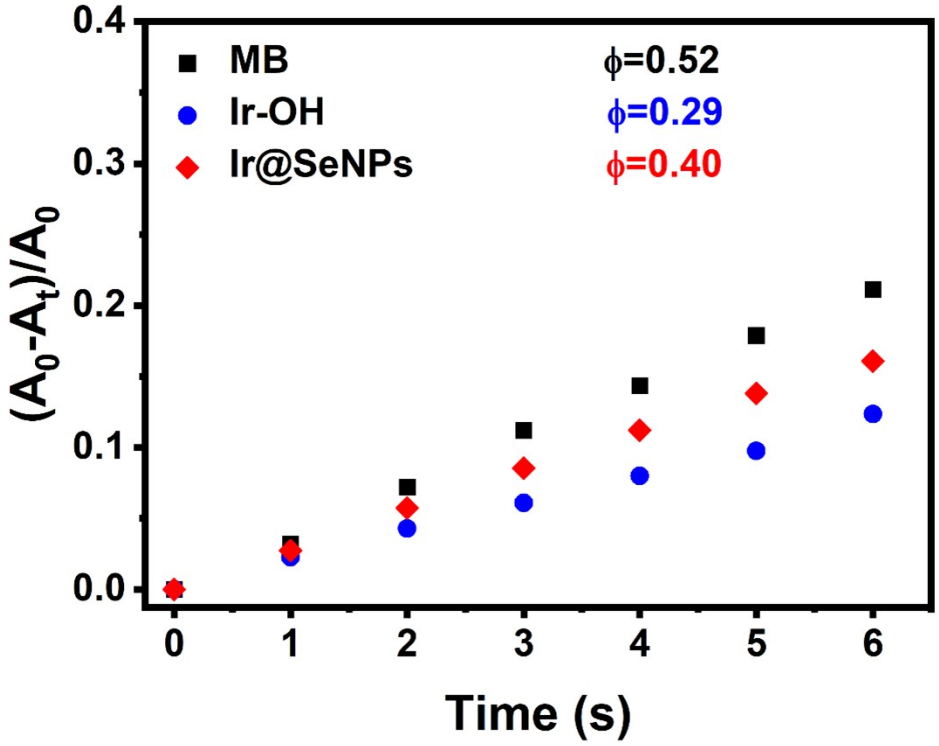

Figure S10. Change in absorption of DPBF at 410 nm upon incubation with **Ir-OH**, **Ir@SeNPs** and Methylene blue (MB) ($OD_{405\ nm}$ = 0.12) and exposure to light irradiation (405 nm, 20 mW cm^{-2}). ϕ represented corresponds to the singlet oxygen quantum yield.

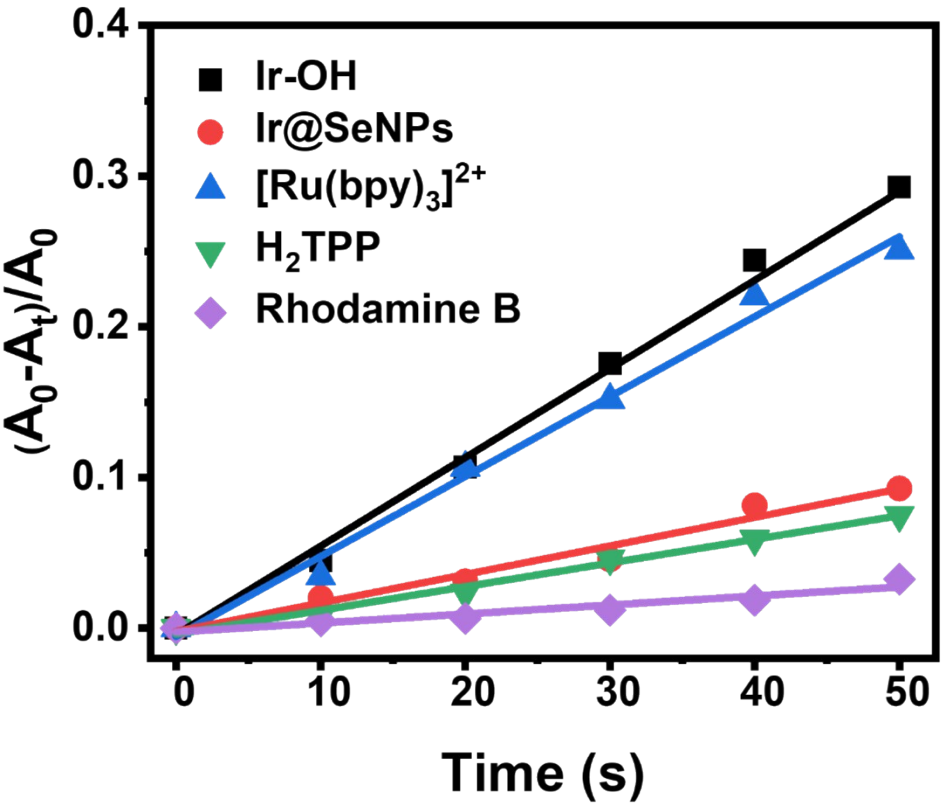

Figure S11. Change in absorption of DPBF at 410 nm upon incubation with **Ir-OH**, **Ir@SeNPs**, $[Ru(bpy)_3]^{2+}$, H_2TPP and Rhodamine B ($OD_{405\,nm}$ = 0.12) under two-photon light irradiation (405 nm, 50 mW) for different time intervals. The line corresponded to the compounds' linear fitting curves.

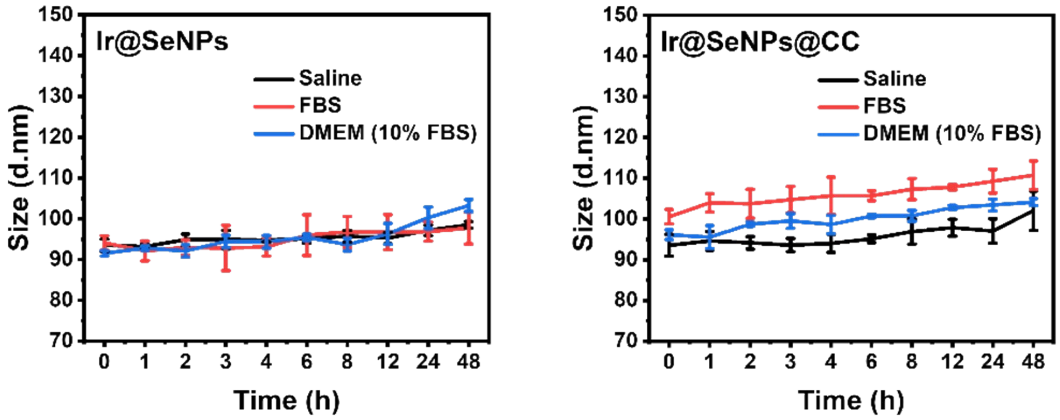

Figure S12. Monitoring of the hydrodynamic diameter of **Ir@SeNPs** and **Ir@SeNPs@CC** in saline, FBS or DMEM supplemented with 10% FBS from 0-48 h.

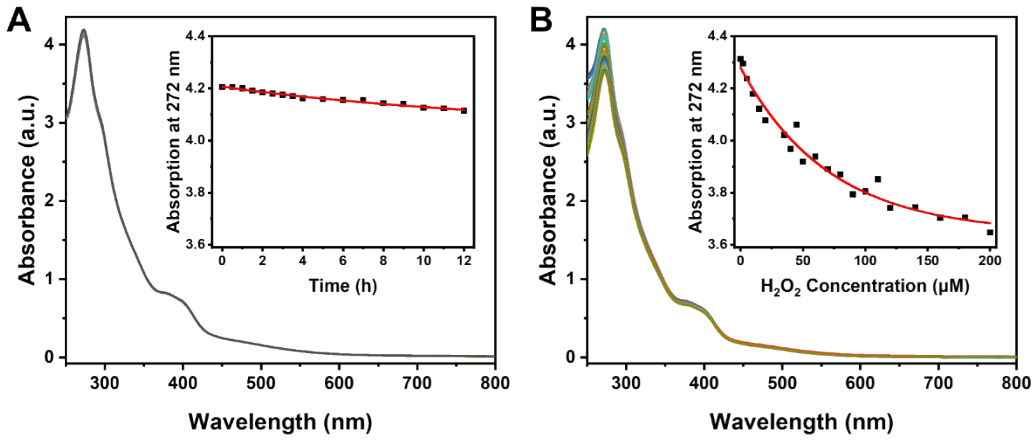

Figure S13. (A) Changes of the absorption of **Ir@SeNPs** ([Ir] = 20 μM) in the absence of H_2O_2 in PBS/CH_3OH (9/1, v/v) from 0-12 h, inset: changes of absorption at 272 nm. (B) Changes in the absorption of **Ir@SeNPs** ([Ir] = 20 μM) upon treatment with H_2O_2 in PBS/CH_3OH (9/1, v/v) from 0-200 μM H_2O_2, inset: changes of absorption at 272 nm.

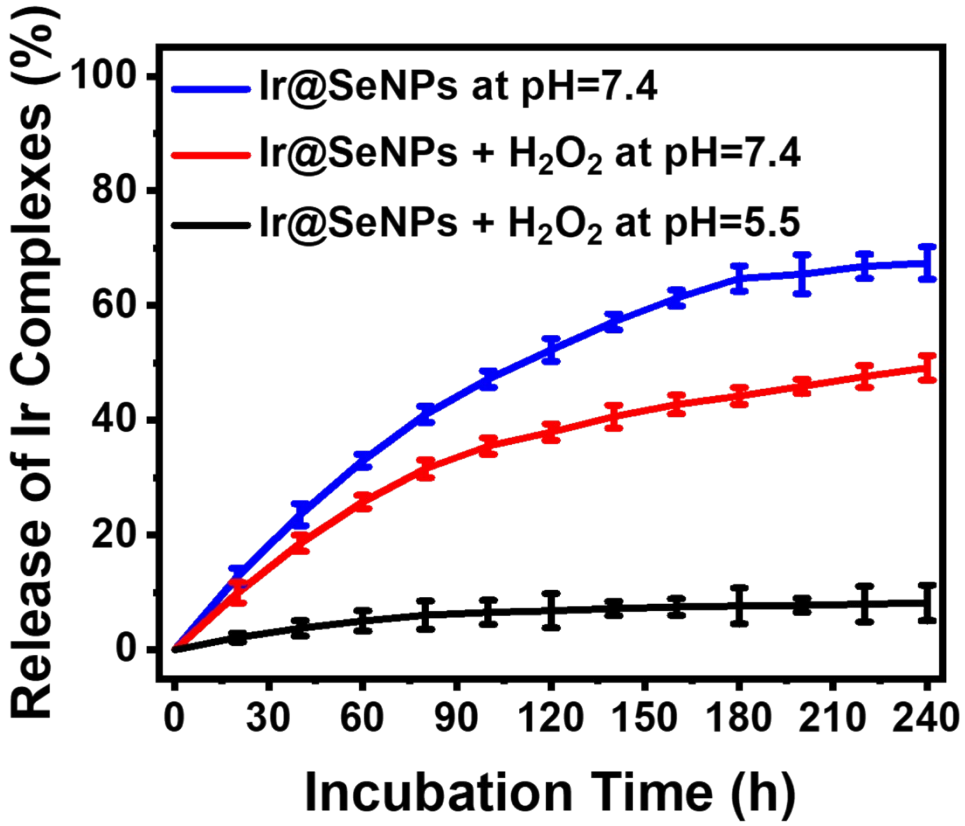

Figure S14. Release kinetics of **Ir@SeNPs** ([Ir] = 20 μM) at pH=7.4, pH=7.4 + 100 μM H_2O_2, or pH=5.5 + 100 μM H_2O_2 measured by ICP-MS (n = 3).

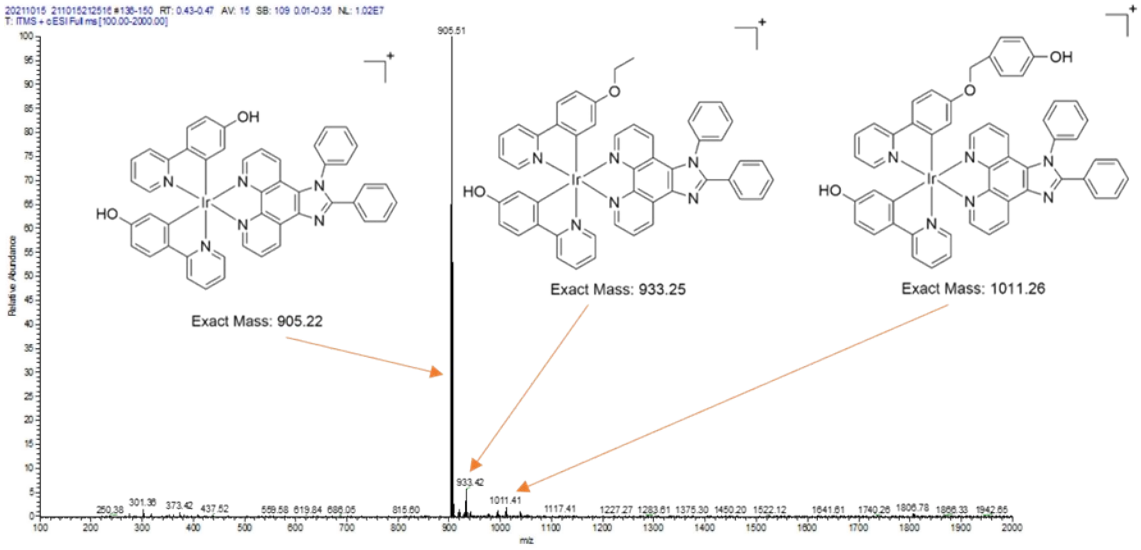

Figure S15. ESI-MS spectrum of the treatment of **Ir@SeNPs** with H_2O_2 under acidic condition (pH=5.5) for 24 h.

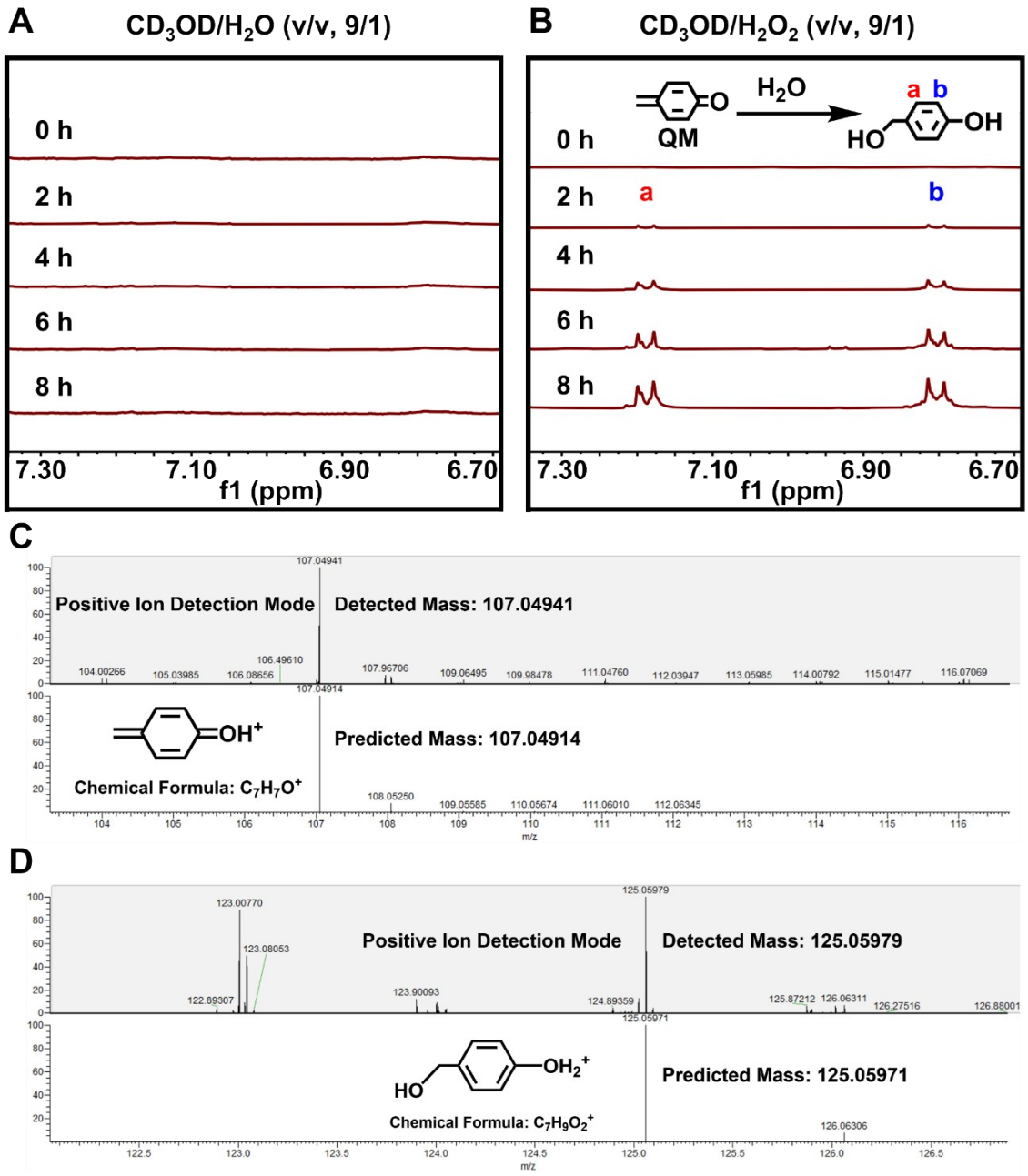

Figure S16. Changes in the ^{1}H-NMR spectra upon incubation of **Ir@SeNPs** with H_2O (A) or H_2O_2 (B) in CD_3OD for various time intervals. HRMS detection of methylquinone (C) and its hydrolysis form (D).

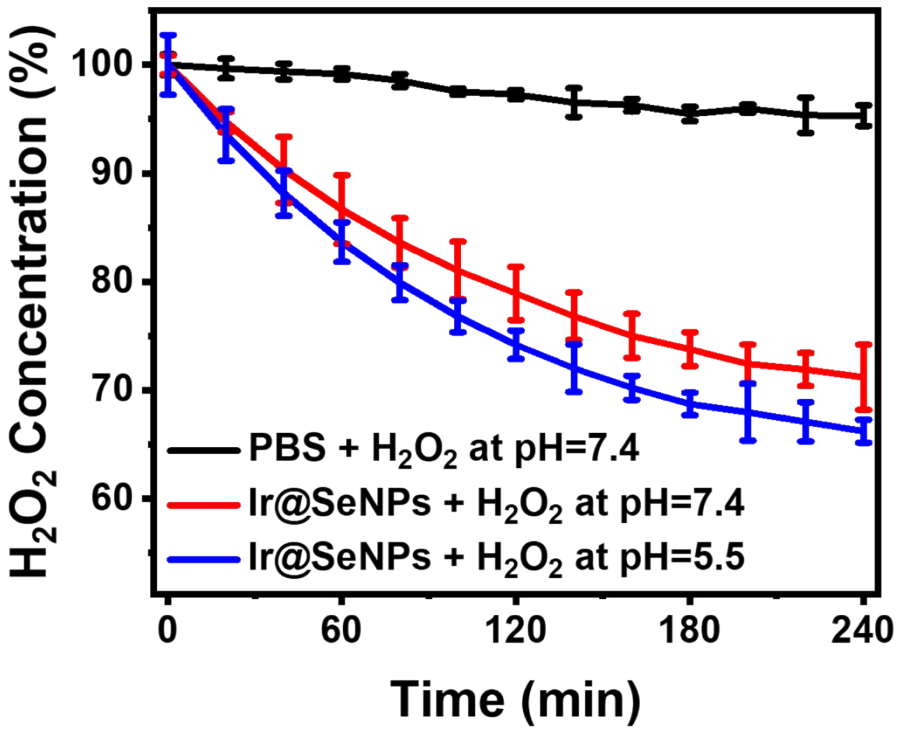

Figure S17. Degradation of H_2O_2 (100 μM) in the presence of **Ir@SeNPs** ([Ir] = 20 μM) under different treatments from 0-240 min (n = 3).

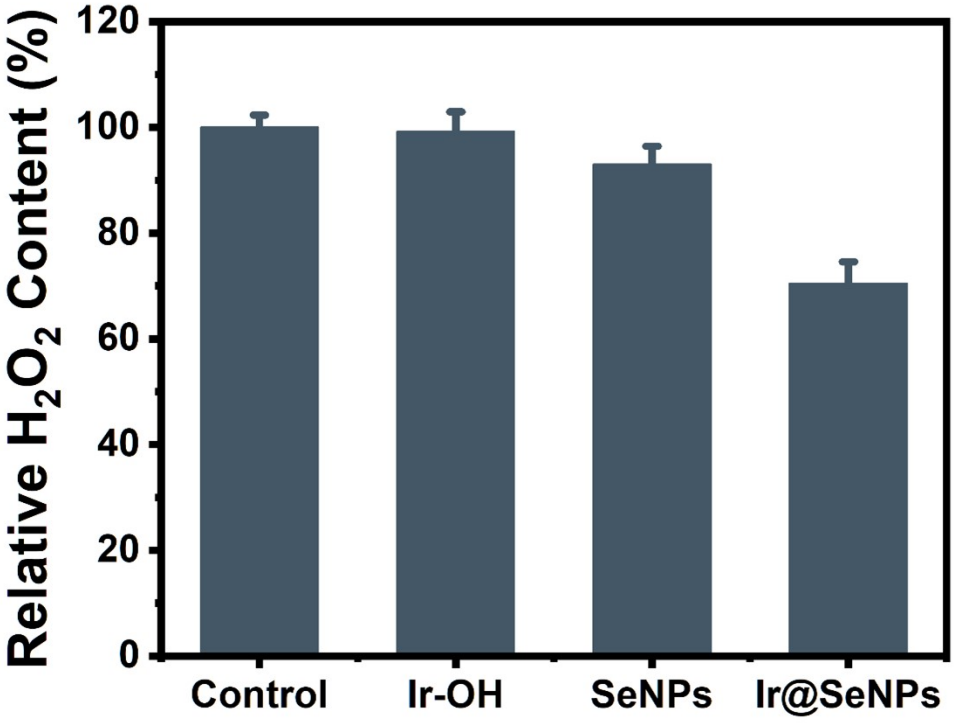

Figure S18. Relative intracellular H_2O_2 levels of A375 cells upon treatment with **Ir-OH, SeNPs**, and **Ir@SeNPs** ([Ir] = 10 μM, [Se] = 20 μg mL^{-1}).

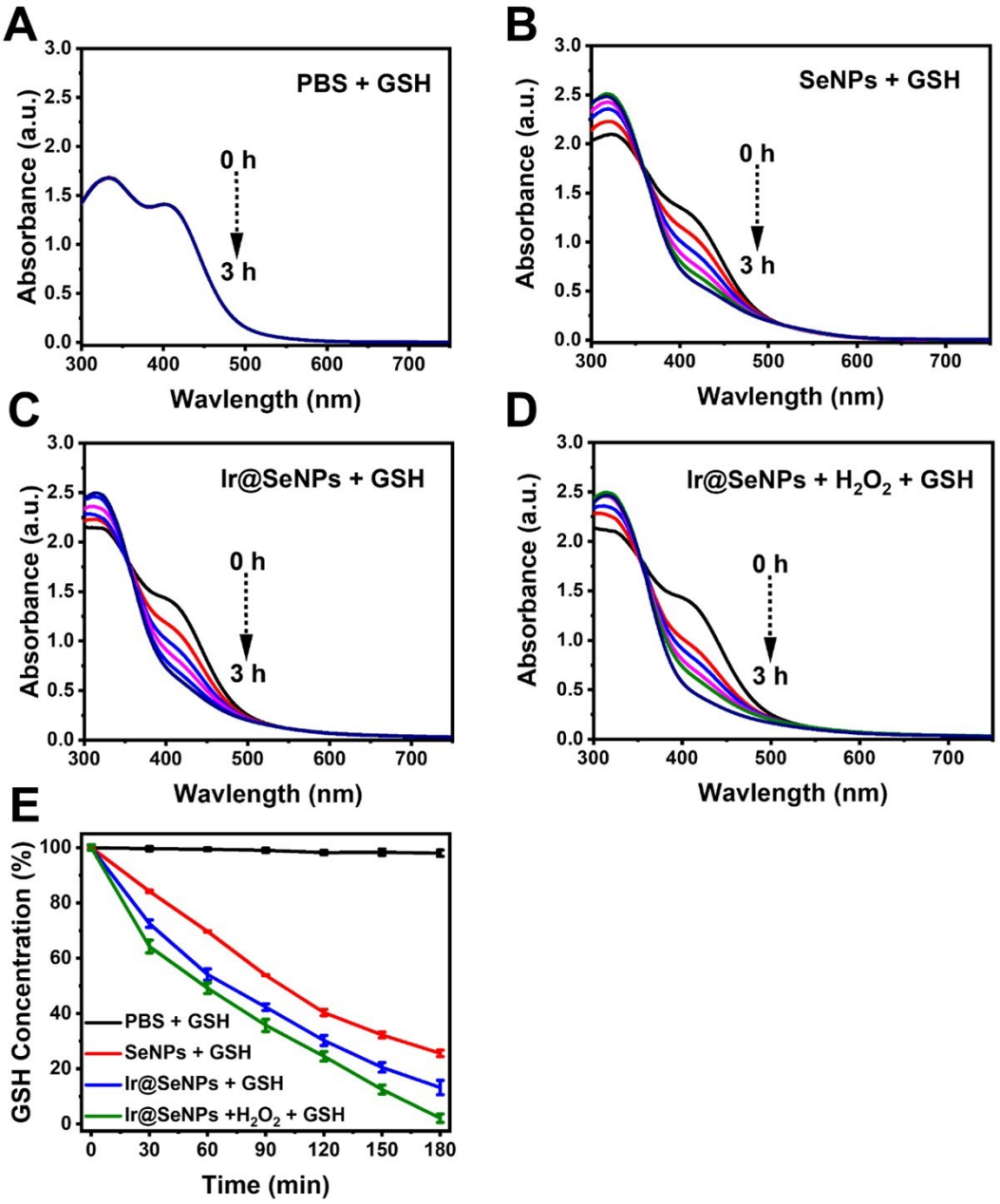

Figure S19. Time-dependent UV absorption spectra of the consumption of GSH (1.0 mM) using the GSH specific probe DTNB at 412 nm upon treatment with (A) PBS, (B) **SeNPs**, (C) **Ir@SeNPs**, and (D) **Ir@SeNPs** that were preincubated with H_2O_2 (500 µM) for 30 min ([Se] = 400 µg mL^{-1}) from 0-3 h. Their GSH depletion (E) was quantified by using the UV absorption decrease at 412 nm (n=3).

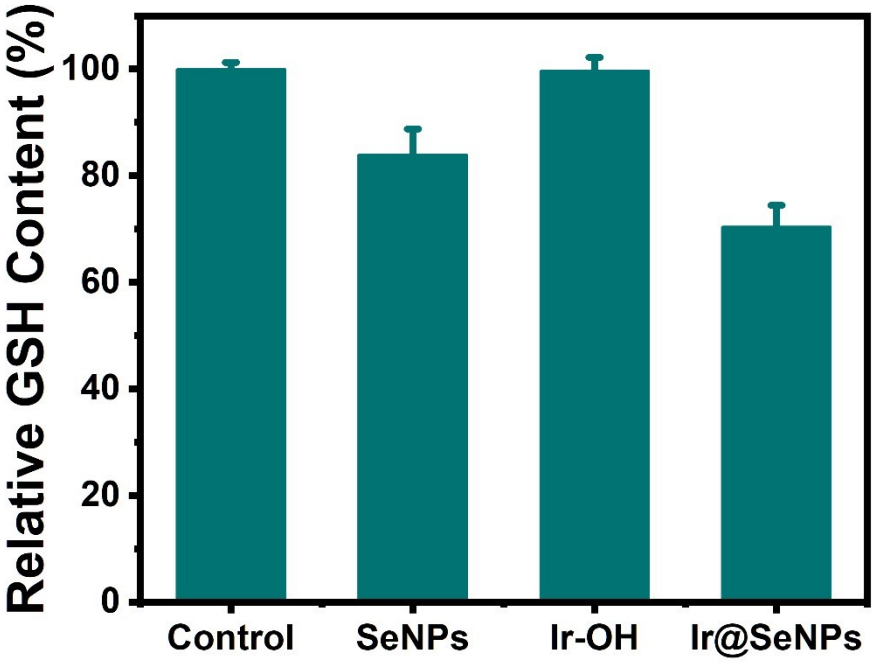

Figure S20. Relative intracellular GSH level of A375 cells upon treatment with **Ir-OH, SeNPs**, and **Ir@SeNPs** ([Ir] = 10 μM, [Se] = 20 μg mL^{-1}).

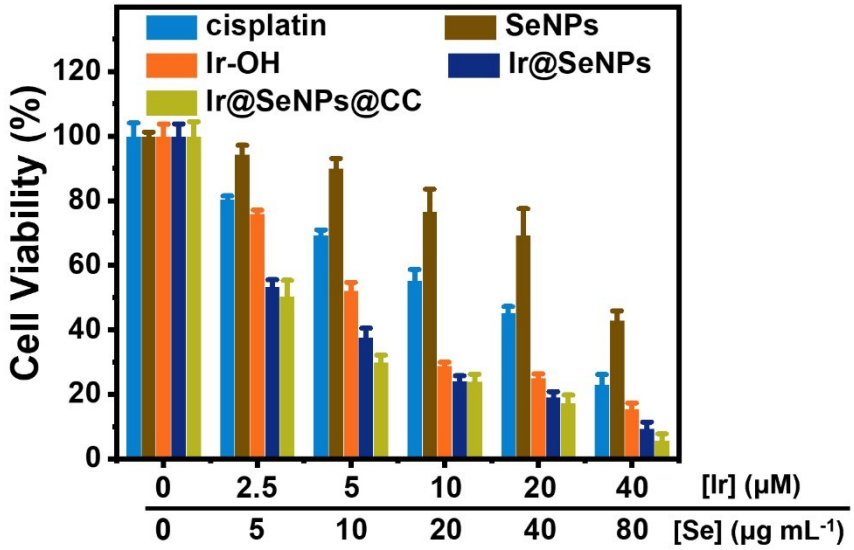

Figure S21. Cytotoxicity of A375 cells incubated with cisplatin, **SeNPs**, **Ir-OH**, **Ir@SeNPs**, and **Ir@SeNPs@CC** ([Ir] = 0-40 μM, [Se] = 0-80 μg mL^{-1}) upon light irradiation (405 nm, 20 mW cm^{-2}, 10 min) (n = 3).

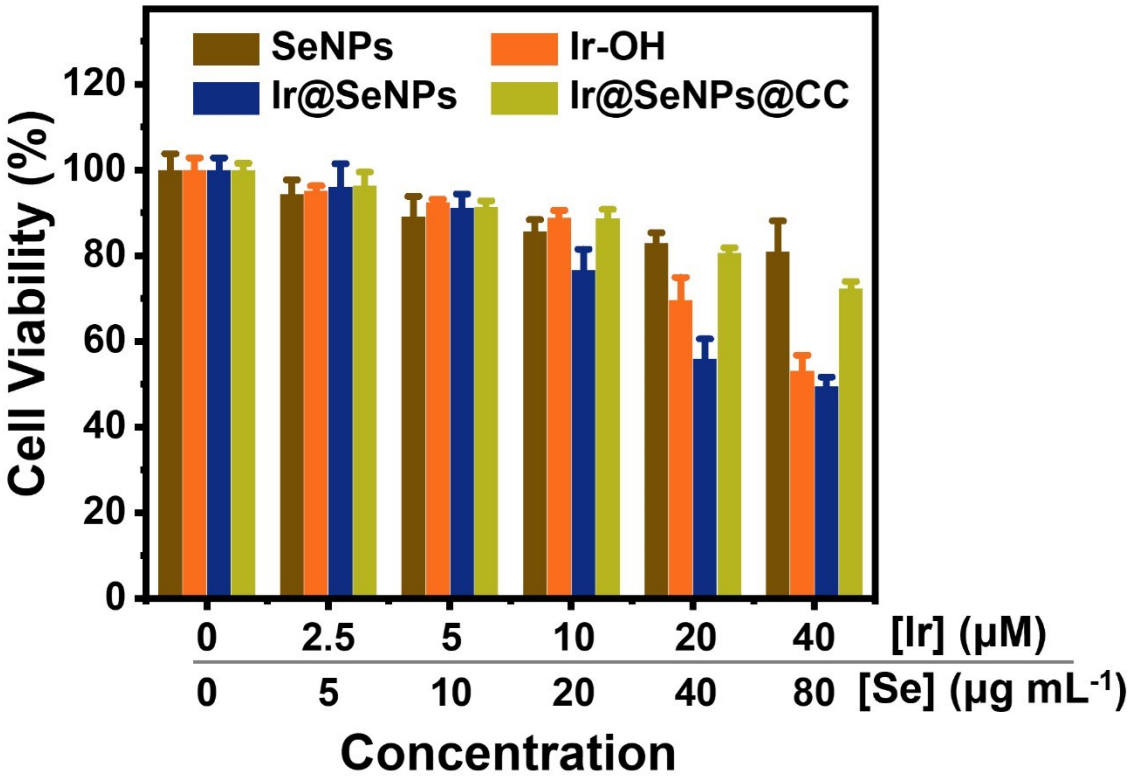

Figure S22. Dark cytotoxicity of L02 cells incubated with **SeNPs, Ir-OH, Ir@SeNPs**, and **Ir@SeNPs@CC** ([Ir] = 0-40 μM, [Se] = 0-80 μg mL^{-1}).

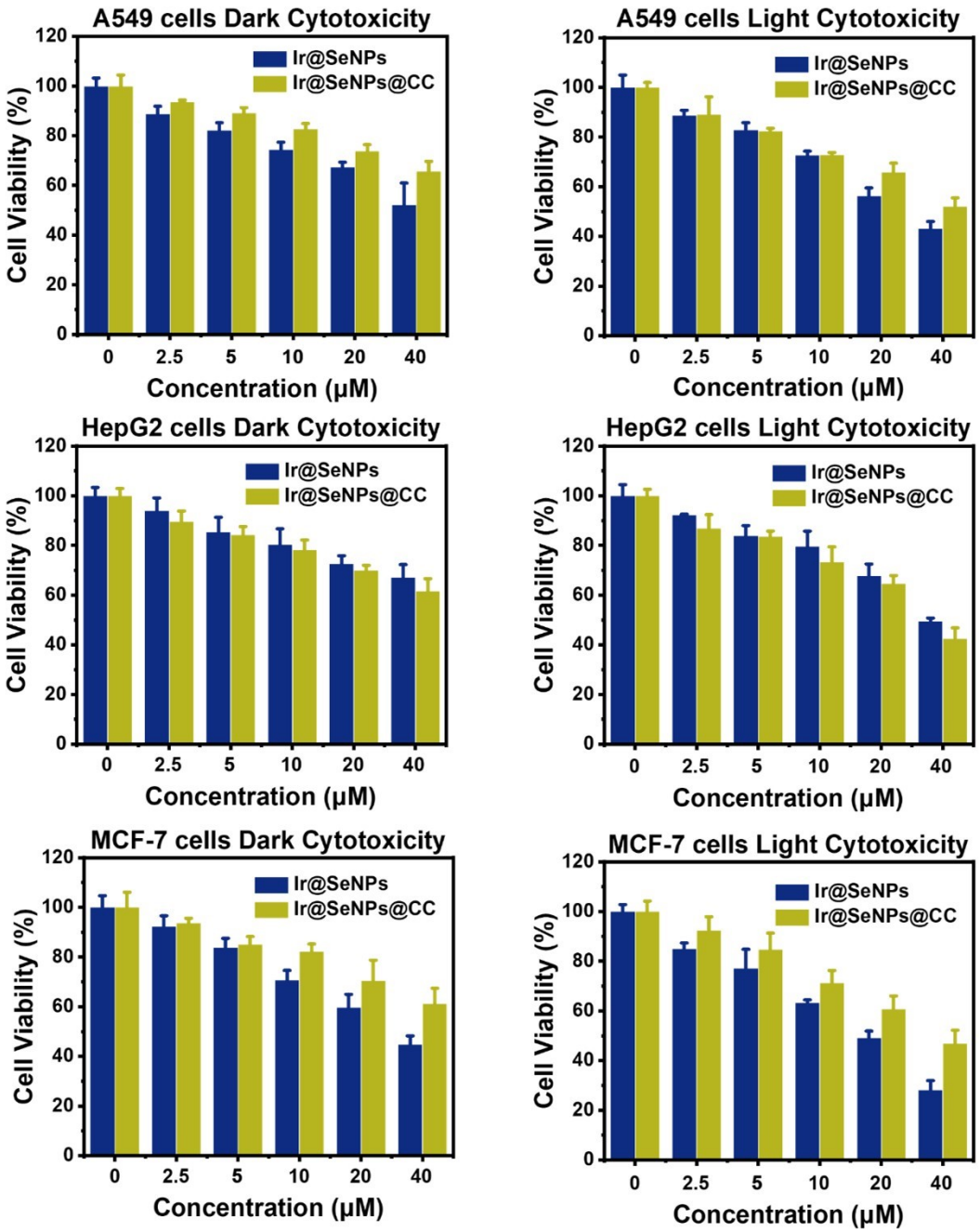

Figure S23. The cytotoxicity of **Ir@SeNPs** and **Ir@SeNPs@CC** ([Ir] = 0-40 μM, [Se] = 0-80 μg mL^{-1}) towards A549 cells, HepG2 cells and MCF-7 cells under dark or light irradiation (405 nm, 10 mW cm^{-2}, 10 min) (n = 3).

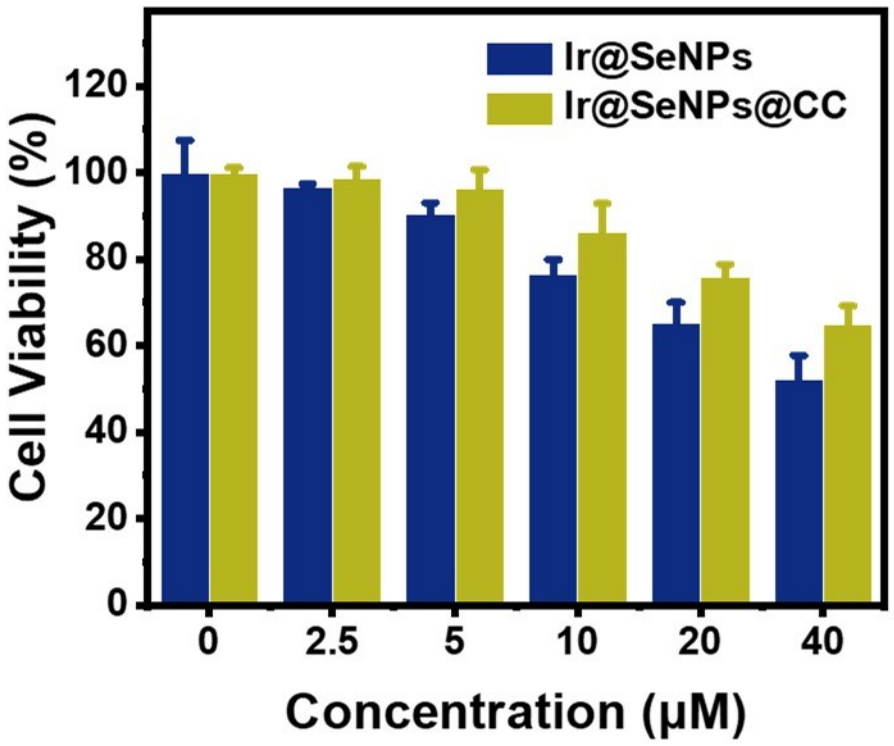

Figure S24. Dark cytotoxicity of RAW 264.7 cells incubated with **Ir@SeNPs** and **Ir@SeNPs@CC** ([Ir] = 0-40 μM).

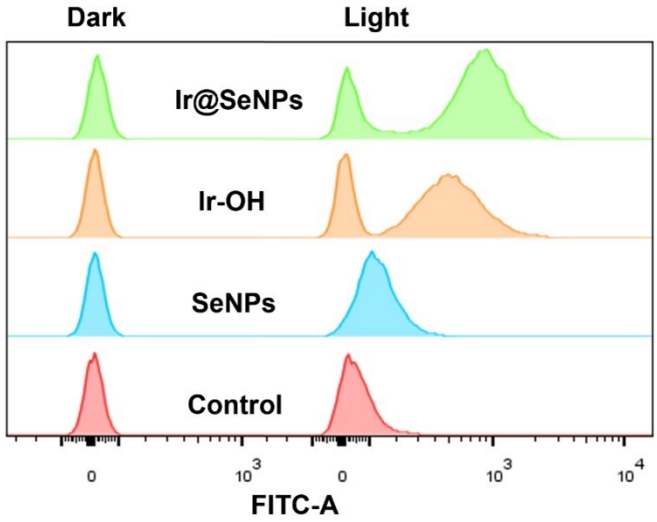

Figure S25. Flow cytometry analysis of A375 cells incubated with **Ir-OH, SeNPs**, and **Ir@SeNPs** ([Ir] = 20 µM, [Se] = 40 µg mL^{-1}) in dark or light irradiation (405 nm, 10 mW cm^{-2}, 10 min) and stained with DCFH-DA.

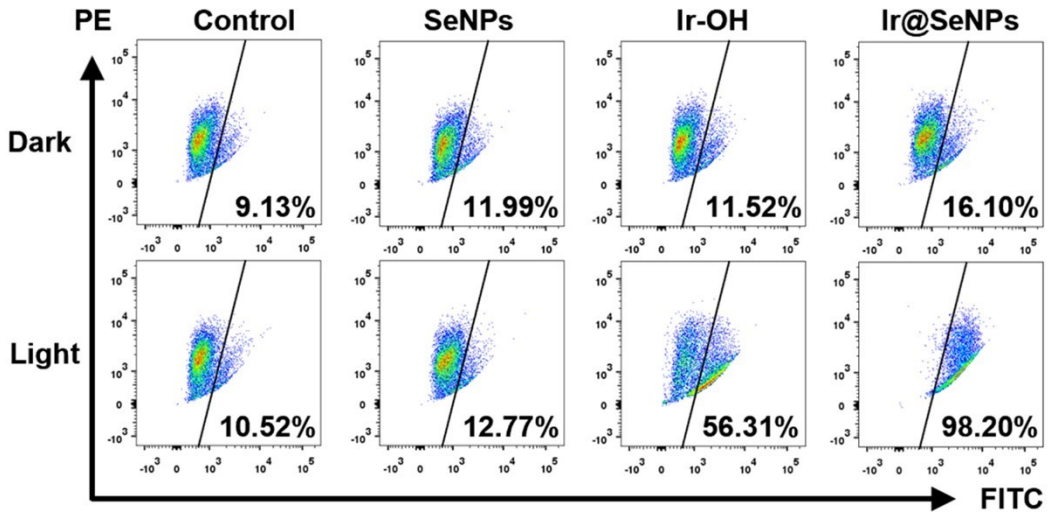

Figure S26. Flow cytometry analysis of A375 cells incubated with **Ir-OH, SeNPs**, and **Ir@SeNPs** ([Ir] = 20 μM, [Se] = 40 μg mL^{-1}) in dark or light irradiation (405 nm, 10 mW cm^{-2}, 10 min) and stained with the mitochondria membrane potential probe JC-1.

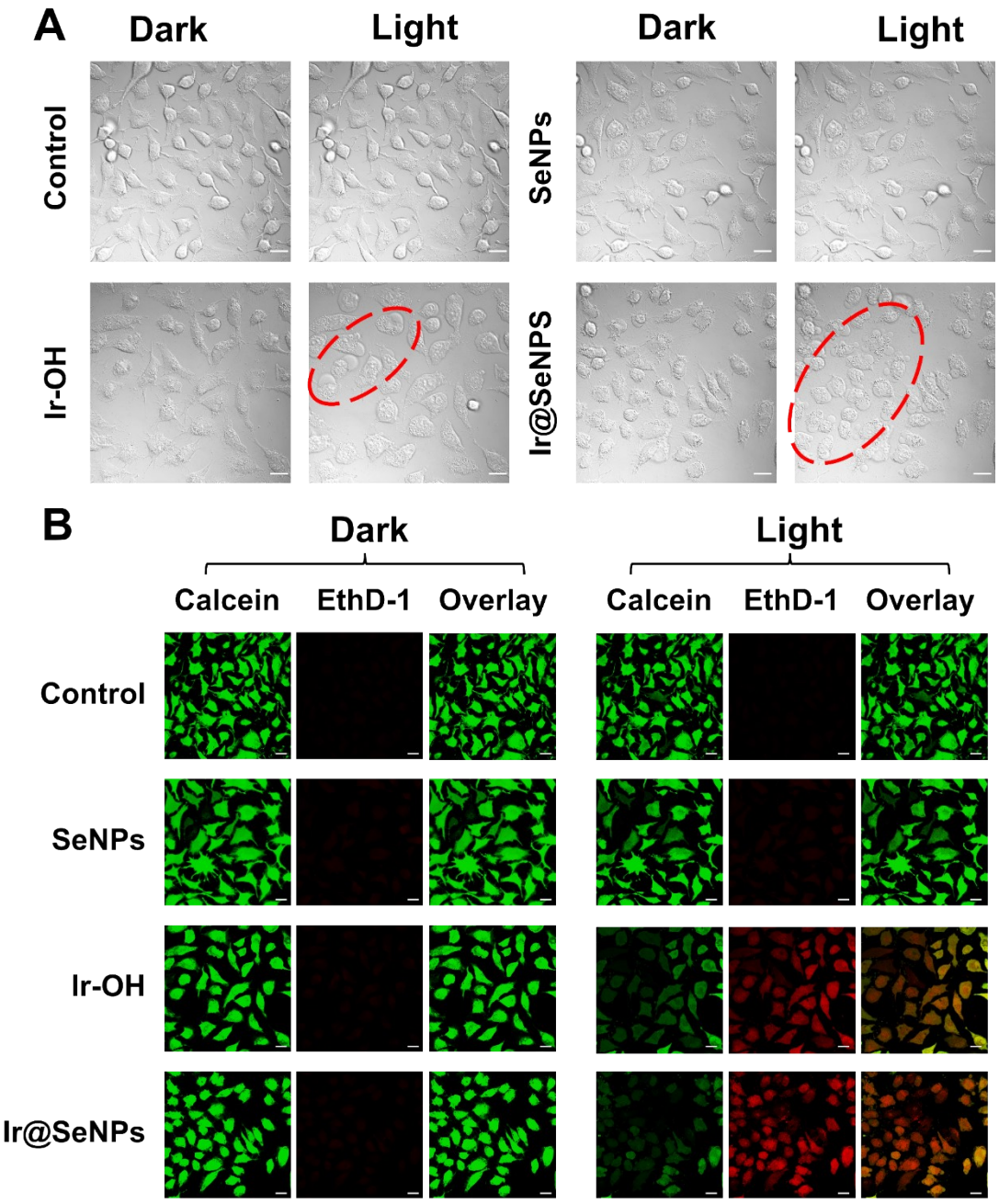

Figure S27. The morphology changes (A) of A375 cells incubated with **Ir-OH**, **SeNPs**, and **Ir@SeNPs** ([Ir] = 20 μM, [Se] = 40 μg mL^{-1}) before and after two-photon irradiation (730 nm, 20 mW, 5 min), and the relative live (Calcein-AM, green)/death (EthD-1, red) staining (B). Scale bar: 20 μm.

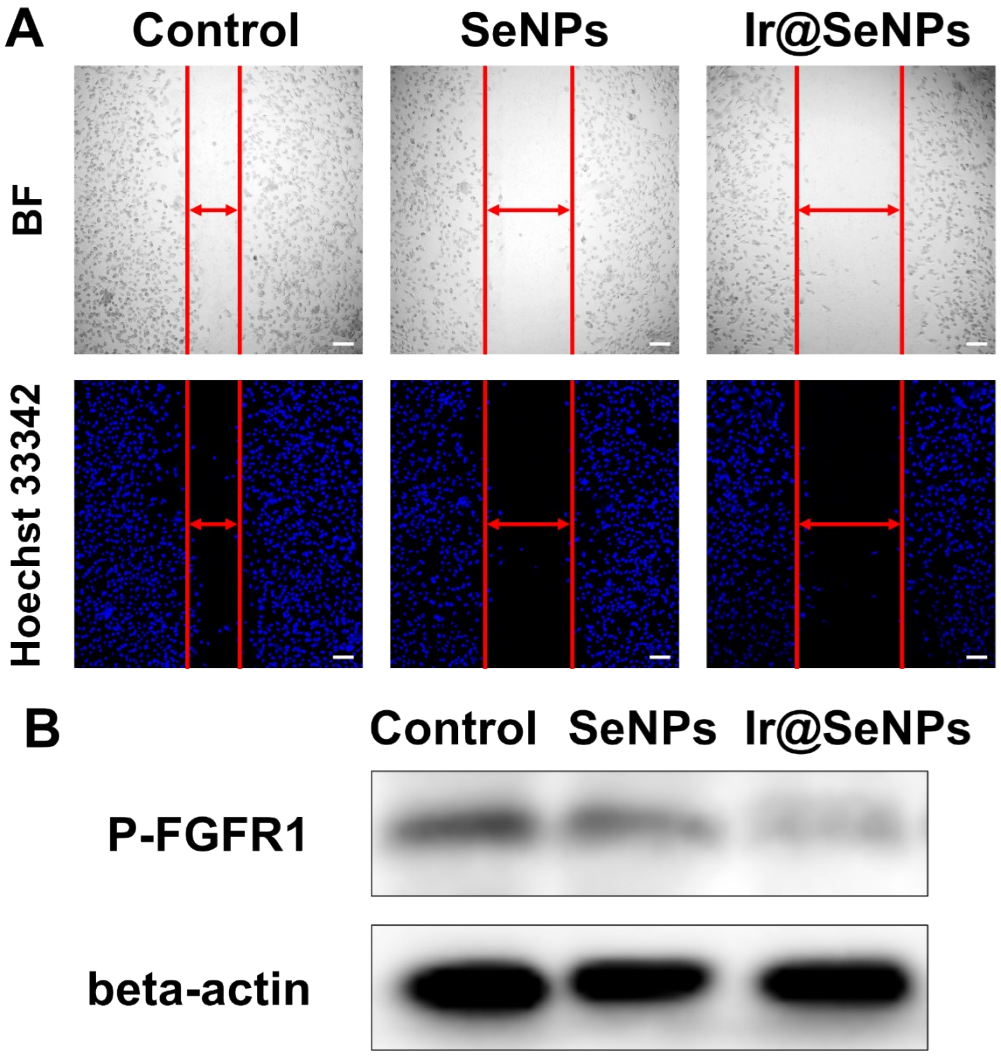

Figure S28. (A) Effects of **SeNPs** or **Ir@SeNPs** on A375 cells migration in wound migration assays (top: bright field, bottom: Hoechst 33342 stained). Scale bar: 20 μm. Cells were wounded with pipette in the absence or presence of **SeNPs** or **Ir@SeNPs** ([Se] = 20 μg mL^{-1}). Scale bar: 100 μm. (B) Effect of **SeNPs** or **Ir@SeNPs** ([Se] = 20 μg mL^{-1}) on the expression of phosphorylation of FGFR1 was determined by immunoblotting after 24 h treatment of A375 cells. Beta-actin was detected as a loading control.

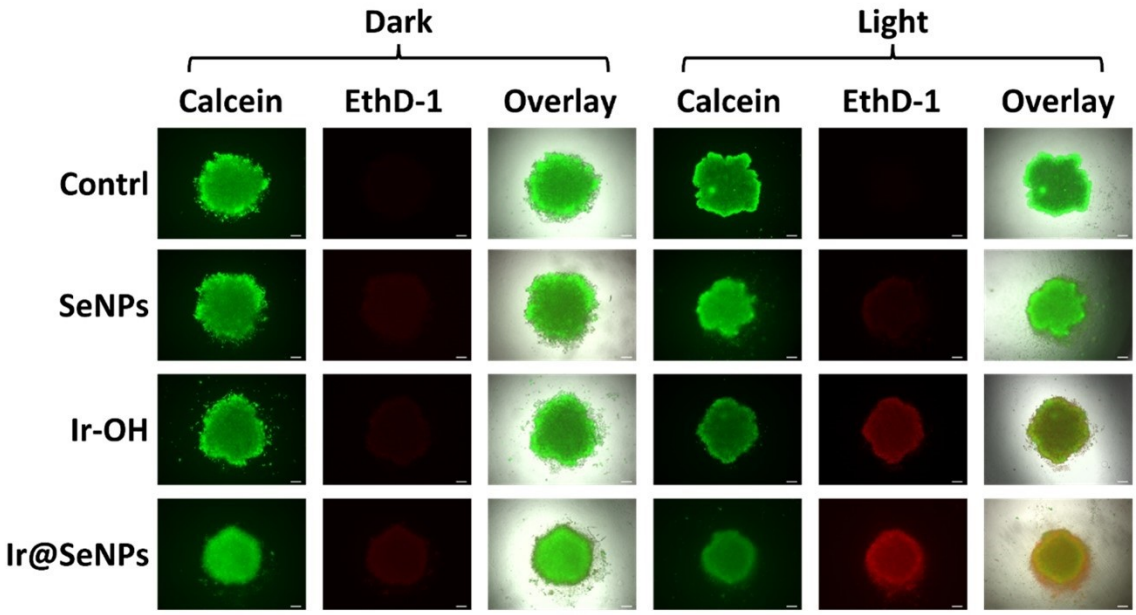

Figure S29. Fluorescence microscopy images of A375 MCTS incubated with **SeNPs**, **Ir-OH,** and **Ir@SeNPs** ([Ir] = 20 μM, [Se] = 40 μg mL^{-1}) upon treatment in the dark or exposure to two-photon irradiation (730 nm, 20 mW, 5 min). The MCTS were stained with Calcein-AM/EthD-1 (Calcein-AM is a stain for living cells, 2μM, λ_{ex} = 488 nm, λ_{em} = 510 ± 10 nm; EthD-1 is a stain for dead cells, 4μM, λ_{ex} = 543 nm, λ_{em} = 610 ± 10 nm). Scale bar = 100 μm.

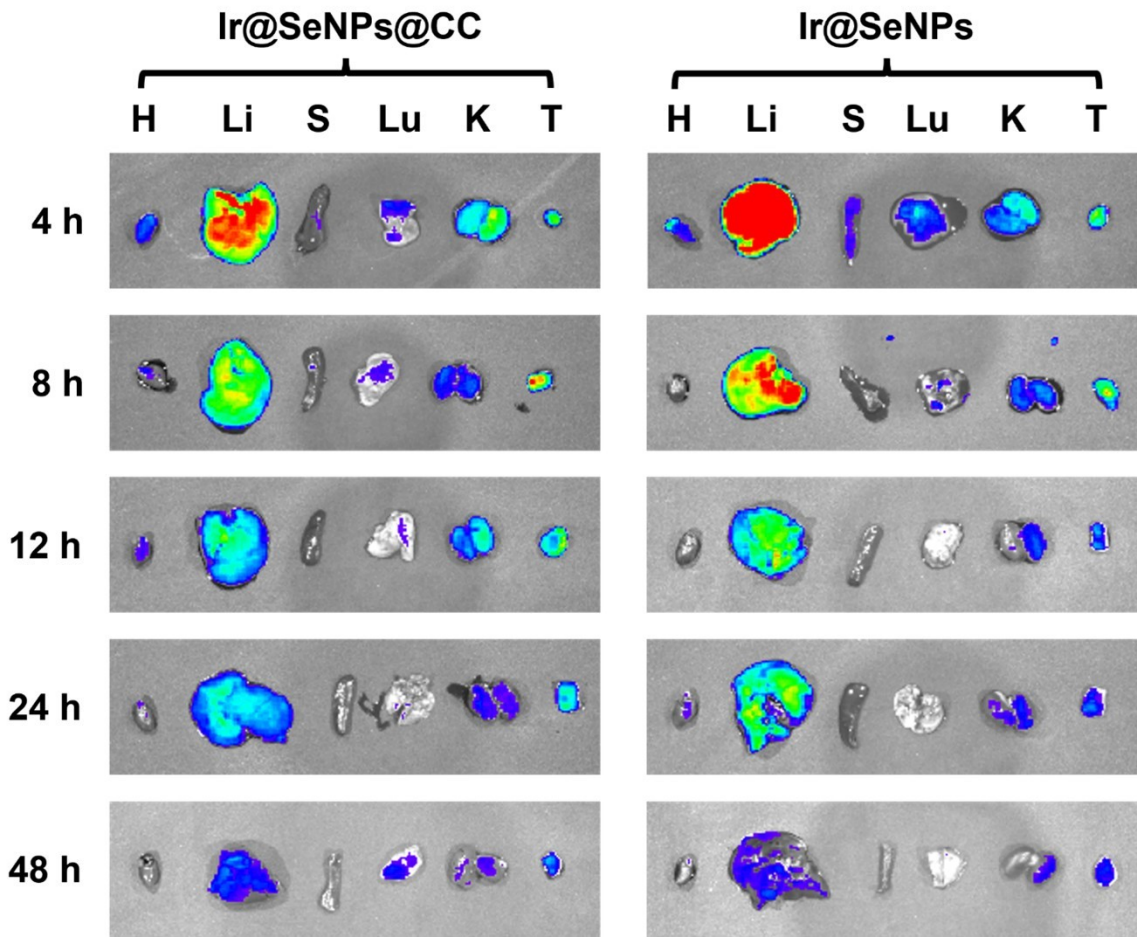

Figure S30. Fluorescence images of the major organs of A375 tumor-bearing mice models after injection with **Ir@SeNPs@CC** or **Ir@SeNPs** (5 mg kg^{-1}) for different periods. H: heart, Li: liver, S: spleen, Lu: lung, K: kidneys, T: tumor. λ_{ex} = 430 nm, λ_{em} = 610 nm.

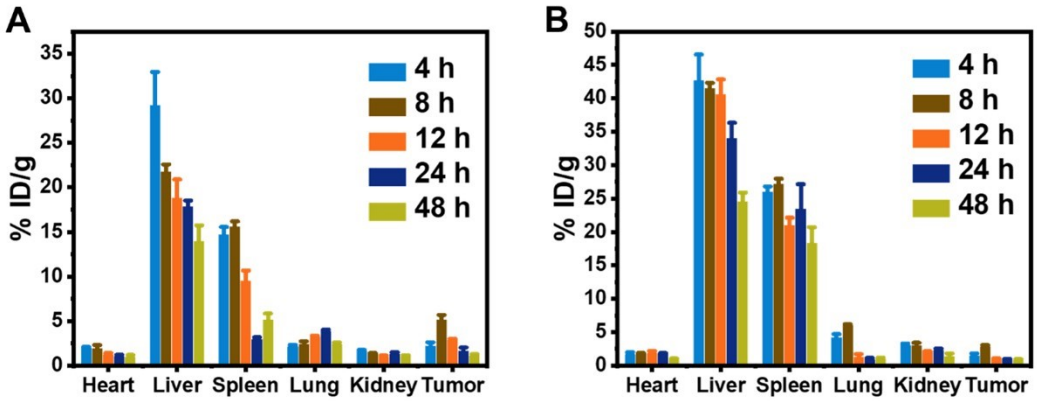

Figure S31. Biodistribution of (A) **Ir@NPs@CC** or (B) **Ir@SeNPs** in major organs and tumors 4, 8, 12, 24 or 48 h after the administration upon determination of the iridium concentration by ICP-MS (n = 3).

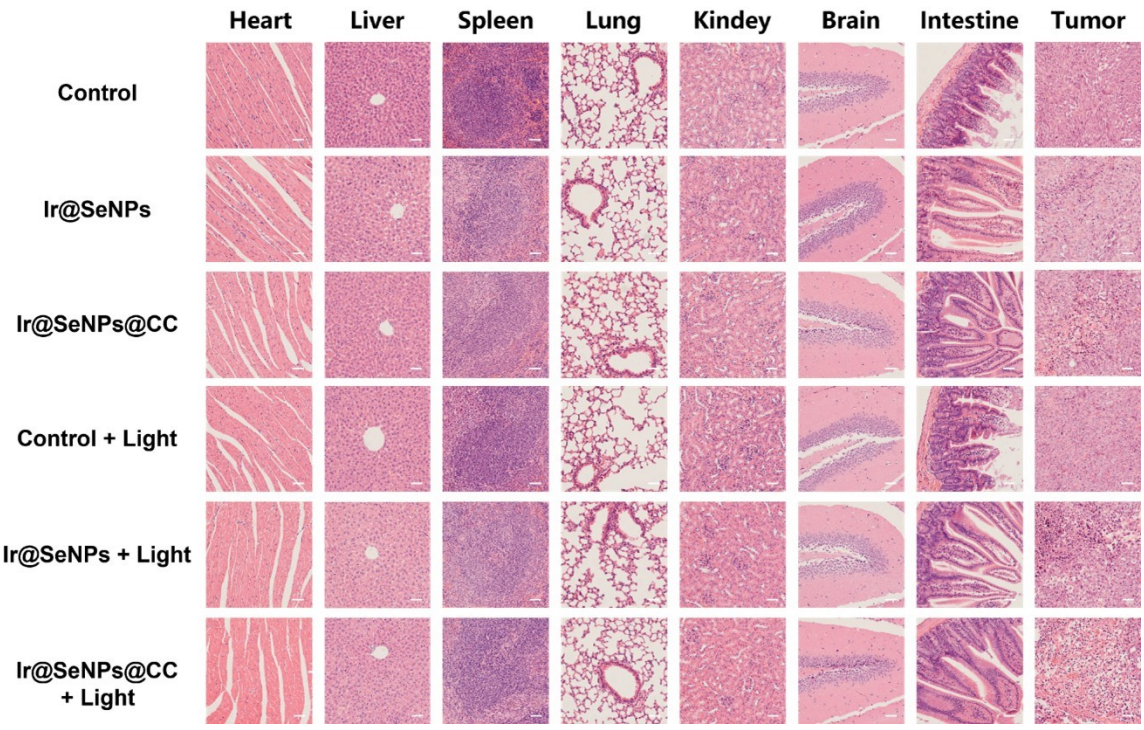

Figure S32. Representative H&E stained histopathologic slices of the major organs and tumors of A375 tumor xenograft mice after various treatments. Light irradiation (λ_{ex} = 730 nm, 50 mW, 5 min). Scale bars: 50 μm.

Table S1. Cytotoxicity towards different cell lines upon 405 nm light irradiation or left in dark (10 mw: 10 mW cm^{-2}, 10 min; 20 mw: 20 mW cm^{-2}, 10 min; PI: photocytotoxicity index) (n = 3).

Compounds		IC_{50}					
		A375 cells	A549 cells	HepG2 cells	MCF-7 cells	RAW 264.7 cells	L02 cells
cisplatin (μM)	Dark	13.2 ± 0.3	-	-	-	-	-
	Light (10 mW)	13.6 ± 0.6	-	-	-	-	-
	PI	1.0	-	-	-	-	-
	Light (20 mW)	13.0 ± 0.5	-	-	-	-	-
	PI	1.0	-	-	-	-	-
SeNPs (μg mL^{-1})	Dark	81.0 ± 1.2	-	-	-	-	300 ± 5.5
	Light (10 mW)	77.0 ± 0.2	-	-	-	-	-
	PI	1.0	-	-	-	-	-
	Light (20 mW)	79.6 ± 0.8	-	-	-	-	-
	PI	1.0	-	-	-	-	-
Ir-OH (μM)	Dark	38.3 ± 0.9	-	-	-	-	100 ± 5.4
	Light (10 mW)	13.2 ± 0.3	-	-	-	-	-
	PI	2.9	-	-	-	-	-
	Light (20 mW)	6.0 ± 0.5	-	-	-	-	-
	PI	6.3	-	-	-	-	-
Ir@SeNPs (μM)	Dark	31.0 ± 1.0	49.4 ± 0.5	87.7 ± 0.7	30.0 ± 0.8	27.8± 3.2	32.6 ± 2.6
	Light (10 mW)	7.5 ± 0.5	29.0 ± 0.6	43.0 ± 1.0	17.0 ± 1.0	-	-
	PI	4.1	1.7	2.0	1.7	-	-
	Light (20 mW)	3.0 ± 0.6	-	-	-	-	-
	PI	10.3	-	-	-	-	-
Ir@SeNPs @CC (μM)	Dark	30 ± 1.8	87.0 ± 1.0	84.2 ± 1.0	66.0 ± 0.2	40.2 ± 2.8	120 ± 8.4
	Light (10 mW)	4.4 ± 0.9	47.0 ± 1.0	34.8 ± 0.5	31.8 ± 0.8	-	-
	PI	6.8	1.8	2.4	2.0	-	-
	Light (20 mW)	2.3 ± 0.2	-	-	-	-	-
	PI	13.3	-	-	-	-	-

Table S2. Cytotoxicity towards A375 MCTS upon 730 nm two-photon light irradiation (730 nm, 20 mW, 5 min) or left in dark (PI: photocytotoxicity index) (n=3).

Compounds		IC_{50}
		A375 MCTS
SeNPs ($\mu g\ mL^{-1}$)	Dark	105 ± 6.0
	Light	97.0 ± 9.2
	PI	1.0
Ir-OH (μM)	Dark	70.0 ± 5.0
	Light	35.3 ± 2.0
	PI	2.0
Ir@SeNPs (μM)	Dark	52.0 ± 2.2
	Light	19.2 ± 1.4
	PI	2.7
Ir@SeNPs@CC (μM)	Dark	45.3 ± 3.8
	Light	10 ± 1.9
	PI	4.5